Influence of ultrasonic vibration honing parameters on cavitation bubble collapse temperature

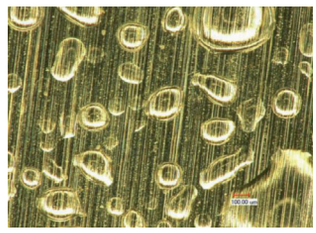

Influencia de los parámetros de pulido por vibración ultrasónica en la temperatura de colapso de las burbujas de cavitación

Xiaoqiang Zhang[1], Xijing Zhu[1*] and Jiangtao Che[2]

[1*] Modern Processing Theory and Technology Research Institute, School of Mechanical and Power Engineering, North University of China, No. 3 Xueyuan Road, Jiancaoping District, 030051, Taiyuan, Shanxi, P.R. China. nuc0741@126.com
[2] School of Mechanical Engineering, Beijing Institute of Technology, No. 5 Nanda Street, Haidian District, 100081, Beijing, P.R. China.

DOI: http://dx.doi.org/10.6036/7979 | Recibido: 29/01/2016 • Aceptado: 06/06/2016

RESUMEN

- La cavitación ultrasónica ha atraído un interés considerable en las aplicaciones industriales del ultrasonido, especialmente sobre su mecanismo y el comportamiento dinámico de las burbujas. Sin embargo, el daño térmico del colapso de las burbujas de cavitación es difícil de estudiar, por su complicado mecanismo. En este trabajo, se analizó el mecanismo de formación de una burbuja de cavitación. Se estableció un modelo dinámico en base al mecanismo de pulido por vibración ultrasónica y se presentó la temperatura de colapso de la burbuja bajo la ley del equilibrio termodinámico. Se estudiaron seis parámetros de pulido (velocidad de rotación de la cabeza pulidora, amplitud de vibración de la onda ultrasónica, velocidad de respuesta del abrasivo, presión de pulido, radio inicial de la burbuja y amplitud de la potencia de la onda ultrasónica) para estudiar la influencia de la variación del radio de la burbuja y la temperatura de colapso. Para los parámetros dados, la variación del radio de la burbuja y la temperatura de fractura se simularon cambiando las condiciones paramétricas de pulido. Los resultados demuestran que el rango de los radios de colapso de las burbujas está entre 100-200 µm y que los valores más altos y más bajos de la temperatura de fractura son 1.400 y 300 ºK respectivamente. La erosión por cavitación en la superficie de una lámina de aluminio corresponde al daño térmico causado por el colapso de las burbujas. Los resultados obtenidos en este estudio aportan valores de referencia para el mecanismo de colapso de cavitación y puede ser aplicado en limpieza ultrasónica, especialmente en la eliminación de capas de óxido.
- **Palabras clave:** pulido por vibración ultrasónica, burbuja de cavitación, temperatura de colapso, erosión por cavitación.

ABSTRACT

Ultrasonic cavitation, particularly its mechanism and bubble dynamic behavior, has attracted considerable interest in industrial ultrasound applications. However, the thermal damage of cavitation bubble collapse is difficult to study because of its complicated mechanism. In this work, the formation mechanism of cavitation bubbles in ultrasonic vibration honing (UVH) was analyzed. A dynamic model was established on the basis of the UVH mechanism, and bubble collapse temperature was presented under the law of thermodynamic equilibrium. Six honing parameters (i.e. rotation speed of the honing head, ultrasonic wave vibration amplitude, reciprocation speed of oilstone, initial bubble radius, ultrasonic wave stress amplitude, and honing pressure) were studied to explore the influence of bubble movement radius and collapse temperature. For the given parameters, the bubble movement radius and crack temperature were simulated by changing the honing parameter conditions. The bubble collapse radius ranged from 100 µm to 200 µm, and the highest and the lowest crack temperatures were 1,400 K and 300 K, respectively. The cavitation erosion on an aluminum foil surface corresponded to the thermal damage caused by the bubble collapse. The conclusions obtained in this study provide significant reference values for the mechanism of cavitation collapse and can be applied in ultrasonic cleaning, particularly in descaling oxide layers.

Keywords: ultrasonic vibration honing, cavitation bubble, collapse temperature, cavitation erosion.

1. INTRODUCTION

Ultrasonic vibration honing (UVH), which is a new processing technology that features low temperature, pulse nature, small cutting force, etc., has been widely researched and developed. The main purpose is to promote the surface quality and to form the overlapping curve which can promote the lubricity of workpiece[1]. In addition, it can extend the working life. The UVH belongs to a meterial removing process which is different from the polish. Fig. 1 shows the machining result of the UVH. The cavitation is a common phenomenon which exists in fluid dynamics and presents different effects in various conditions. The main behavior is shown in hydrodynamic cavitation and acoustic cavitation, and many relevant studies have been conducted by scholars and professionals from all over the world [2-5]. Ultrasonic cavitation, induced by ultrasonic waves and produced in honing zones, is a physical phenomenon. An ultrasonic wave, which is the main fac-

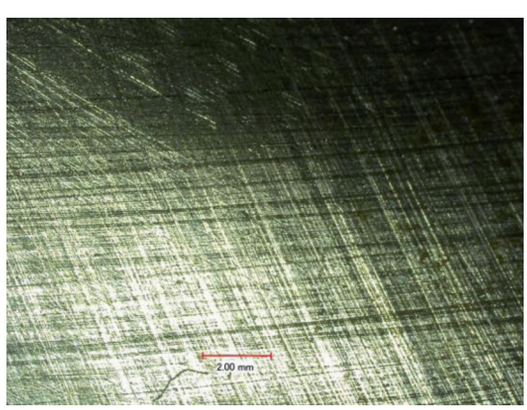

Fig. 1: The machining result of UVH

tor to induce cavitation bubbles, is produced by a supersonic generator and is transmitted by an ultrasonic transducer, a booster, a bending vibration disk, and a flexible string to an oilstone. Finally, negative pressure is generated in the cooling liquid, and cavitation bubbles are induced.

The bubble oscillates in the cooling liquid because of the ultrasound effect, and the energy is collected inside the bubble. After several periods of oscillation, the bubble collapses, and the energy is released. High-temperature and high-pressure apraying is performed, and the workpiece surface is impacted. Cavitation thermal damage is formed, and different cavitation erosions appear on the surface. Bubble dynamics, including single and multiple bubbles, has been studied in detail, but the heat effect of bubble collapse has been ignored to simplify analyses. Therefore, a bubble collapse model should be established, and the heat effect brought by bubble collapse in ambient temperature, particularly on workpieces, should be analyzed.

2. STATE OF THE ART

The first cavitation bubble dynamic model was developed by Rayleigh [6] and then was extended by Plesset [7]; the Rayleigh-Plesset (RP) equation was obtained thereafter. This equation has been the foundation of studies on this topic. For hydrodynamic cavitation, Cai et al. [8] proposed an interaction model of bubbles in a venture cavitation reactor on the basis of the RP equation. Furthermore, the influence of ambient factors, such as liquid temperature, cavitation number, and inlet pressure of venture, on bubble dynamic behavior was analyzed with the fourth-order Rung-Kutta method. The results showed that the bubble radius decreased with liquid temperature and cavitation number increasing and remained stable with inlet pressure increasing. The influence of heat transfer on bubble motion was also investigated on the basis of a spherical gas/vapor bubble. The nonlinear energy method coupled with the RP equation was presented using bifurcation theory and was transformed into an open dynamic engine system. Free and forced oscillations were then simulated and compared. For free oscillations, the damping effect of the heat transfer increased, whereas that of the viscosity decreased with ambient temperature increasing. For forced oscillations, the hysteresis was significant. Three types of numerical methods were compared to evaluate the efficiency of heat transfer [9]. To investigate cavitation damage, Matevž Dular et al. [10] studied cavitation damage in hydrodynamic environments and discussed their specific degrees at elevated temperatures. The micro-jet theory and spherical bubble collapse theory were investigated on the basis of the experiment and evaluation, with the temperature influence on the former being marginal. The experiment was conducted on polished aluminum samples, and the significant temperature was determined to be 60 °C. The ambient temperature was considered for bubble moving motion. Despite these research efforts, the influence of heat exchange has largely been ignored. Therefore, a wide range of studies related to the heat aspects of the bubble motion problem, namely, cavitation dynamics, bubble collapse, and collapse temperature, have been conducted [11-15]. Such studies aimed at improving the bubble dynamic model and dynamic motion by considering the effect of thermal transmission. Zhao et al. [16] investigated the cavitation flow in high-pressure and high-temperature environments by combining Singhal's cavitation model with an improved re-normalisation group k-ε turbulence model. The simulation was conducted on a 2D NACA0015 for two different temperatures, and the results were compared. The vaporization latent heat was found to be a significant factor in the high-temperature cavitation process. Moreover, cavity time was relatively short under high-temperature conditions. Balaji Mohan et al. [18] developed a new hybrid spray model by coupling a cavitation model and the KHRT spray model. The experiment was conducted to compare the new model with the non-vaporizing and vaporizing spray models in diesel engines. Laser-induced cavitation, such as the bubble collapse near a rigid boundary, was also investigated [19], and the energy loss from bubble movement was discussed [18].

Acoustic cavitation was then studied. For example, the dynamic model of a single cavitation bubble in UVH was established [20], and two bubbles were developed [21]. Furthermore, the cavitation sound field was simulated and measured [22]. Exact pressure and temperature distributions were discussed by Cogné et al. [23,24] for a single bubble induced by an acoustic wave. Therefore, two different approaches were proposed, and the results showed that the computed result was matched that of the rigorous approach. The nucleation rate and nuclei number of a single collapsing bubble were determined. The effects of ambient parameters were analyzed, and a set of optimal arguments was confirmed. High-frequency bubble characterization was presented by Marc Schlender et al. [25]. Consequently, three characteristic cavitation patterns were found in constant pressure, and the further emulsification experiment was conducted to identify the cavitation pattern. The dynamics of multiple cavitation bubbles in an acoustic field was proposed by Ye Xi et al. [26] by considering compressibility, acoustic wave frequency, amplitude, incident angle, and bubble arrangement. The effect of all factors on bubble dynamics was computed numerically, but the thermal impact was neglected. Mahdi et al. [27] presented the energy loss theory based on the cavitation bubble dynamics by considering fluid compressibility. They found that factors such as cavitation number, initial radius, and hydrofoil angle of attack were significant in thermal radiation heat transfer. However, the study did not consider the thermal process for bubble movement.

As mentioned above, most of the relevant research on cavitation bubbles mainly explore dynamic characteristics, but largely ignore the thermal effect. Thermal damage is significant in the actual machining process. This paper considers the thermal effect in bubble movement and researches the bubble collapse temperature. Experiments are conducted to verify the result of the study.

The remainder of this paper is organized as follows. Section 3 describes the cavitation bubble-generating mechanism and the dynamic model of UVH and presents the experimental preparation. Section 4 provides the analysis results and experimental test results, as well as the detailed discussions. Section 5 summarizes the conclusions.

3. METHODOLOGY

3.1. CAVITATION BUBBLE VIBRATION MODEL

The UVH device is shown in Fig. 2(a). The ultrasonic wave is produced by a supersonic generator and is then directly transmitted into an ultrasonic transducer with a connecting wire. In the ultrasonic transducer, the ultrasound is transformed into axial mechanical vibration. The booster, which is the main part that transfers the vibration, then gathers and magnifies the vibration. Thereafter, a strong mechanical vibration is transmitted to the bending vibration disk and is converted from the axial direction to the radial direction. A flexible string and an oilstone seat

are welded to receive the vibration signal together. An oilstone is bonded to its seat with strong glue. Finally, the oilstone takes the vibration for machining the workpiece.

As a display of the inner structure of the UVH device, Fig. 2(b) shows the fundamental principle of cavitation generation in UVH. The parameters that affect oilstone movement include ultrasonic vibration velocity v_f, device rotation speed v, and reciprocation speed v_a of the oilstone. Thereafter, the speed of the oilstone in honing can be expressed by Eq. (1).

$$v_{ea} = \sqrt{v^2 + (v_a + v_f)^2} = \sqrt{(\pi dn)^2 + (v_a + 2\pi Af\cos 2\pi ft)^2} \quad (1)$$

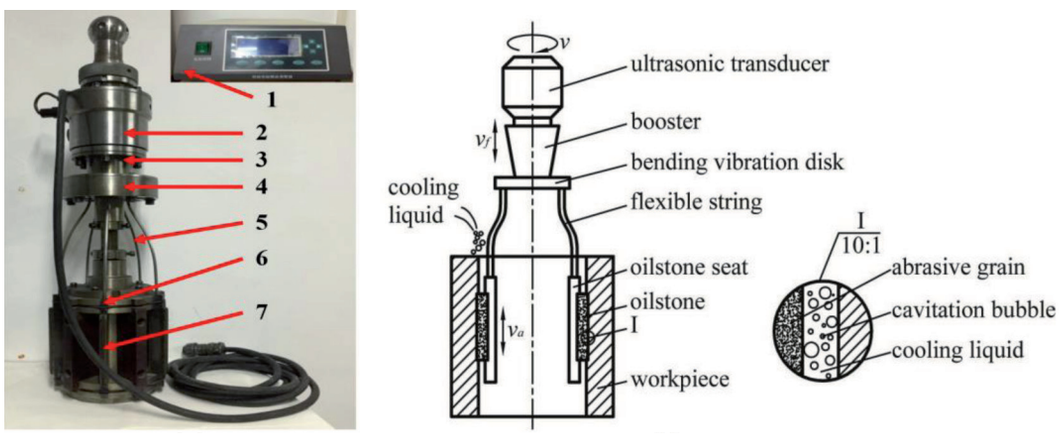

(a) *(b)*

1 - supersonic generator, 2 - ultrasonic transducer, 3 - booster, 4 - bending vibration disk, 5 - flexible string, 6 - oilstone seat, 7 - oilstone
Fig. 2: UVH device and fundamental principle diagram

where n is the rotational speed of the honing device, d is the machining diameter, A is the ultrasonic wave vibration amplitude, and f is the ultrasonic wave vibration frequency.

In the honing zone, the cooling liquid is the basic requirement for cavitation generation and is necessary in machining. Furthermore, cavitation bubbles exist in the honing zone as a free state. On the basis of the classical RP equation [6], the effects of ambient pressure, surface tension, cooling liquid viscosity, honing pressure, honing speed, and ultrasonic pressure are considered. The dynamical governing equation can then be obtained as follows for a single cavitation bubble in UVH.

$$R\ddot{R} + \frac{3}{2}\dot{R}^2 + \frac{3}{2}v_{ea}^2 = \frac{1}{\rho}\left[\left(p_0 + p_v + \frac{2\sigma}{R_0}\right)\left(\frac{R_0}{R}\right)^{3\kappa} - \frac{2\sigma}{R} - p_0 + p_v - p_h + p_a \sin 2\pi ft - \frac{4\mu}{R}\dot{R}\right] \quad (2)$$

where R_0 is the bubble initial radius, ρ is the cooling liquid density, p_0 is the ambient static pressure, p_v is the saturated vapor pressure inside the bubble, σ is the surface tension coefficient of the cooling liquid, p_h is the honing pressure from the oilstone, p_a is the ultrasonic wave stress amplitude, μ is the viscosity of the cooling liquid, and κ is the gas polytropic index.

The following assumptions are used for simplifying the model:

(1) The bubble remains global in its movement.
(2) The gas inside the bubble exists in the form of water vapor.
(3) The ambient liquid for the cavitation bubble is incompressible.
(4) The chemical reaction occurring inside the bubble is ignored.

3.2. CAVITATION BUBBLE COLLAPSE TEMPERATURE

In UVH processing, high temperature and high pressure are developed after a series of aerodynamic processes. However, the cavitation bubble maintains a steady thermodynamic equilibrium. The inner vapor inside the bubble is assumed to be water vapor. In a high-temperature condition, the state equation can be expressed as follows:

$$p_v(T_v, \rho_v) = \frac{\rho_v B_v T_v}{1 - b_1\rho_v} - b_2\rho_v^2 \quad (3)$$

$$\varepsilon(T_v, \rho_v) = \frac{B_v T_v}{\gamma - 1} - b_2\rho_v \quad (4)$$

where ε, ρ_v, and T_v are the inner energy, density, and temperature of water vapor, respectively; B_v = 458.9 is the gas constant; and γ, b_1, and b_2 are constants.

The cavitation bubble obtains the energy from the ambient pressure in the course of bubble generation to collapse. The energy is expressed as follows:

$$E_b = -p_0\int_{R_0}^{R_s} 4\pi R^2 dR \quad (5)$$

where R_s and R_0 are the bubble collapse radius and initial radius, respectively.

In this study, the vapor density is assumed to remain unchanged, that is, it coagulates under vibration. The released energy for vapor coagulating is written as:

$$E_v = \frac{4}{3}\pi\left(R_0^3 - R_s^3\right)\rho_{v0} l_v \quad (6)$$

where ρ_{v0} and l_v are the saturated density and condensation heat of vapor, respectively, at T_0 = 296.15 K.

In the procedure, the energy for the uncondensed vapor to transform from the initial temperature to the critical collapse temperature is obtained as follows:

$$E_a = \frac{4}{3}\pi R_s^3\rho_{v0}\Delta\varepsilon = \frac{4}{3}\pi R_s^3\rho_{v0}\frac{B_v}{\gamma - 1}(T_c - T_0) \quad (7)$$

where T_c is the critical temperature for bubble collapse; $\Delta\varepsilon = \varepsilon(T_c, \rho_{v0}) - \varepsilon(T_0, \rho_{v0})$.

On the basis of the energy conservation principle, the following equation can be obtained:

$$E_b + E_v = E_a \quad (8)$$

Based on Eqs. (5), (6), (7), and (8), the critical temperature of bubble collapse is given by the following:

$$T_c = \frac{\left(p_0 V_0 - p_0 V_s - V_s \rho_{v0} l_v + V_0 \rho_{v0} l_v\right)(\gamma - 1)}{V_s \rho_{v0} B_v} + T_0 \quad (9)$$

The bubble vibrates in honing process and a lot of energy is collected inside. When the bubble collapses after a series of dynamic behaviors, the energy of high temperature and high pressure is released. The workpiece is impacted by the high temperature and the thermal damage is formed on the workpiece surface. Based on the Eq. (9), the bubble collapse temperature can be calculated. Furtherly, the thermal damage temperature on surface can be obtained by the material gasifying energy.

3.3. MATERIAL GASIFYING TEMPERATURE CALCULATION

The aluminum foil is chosen as the test material for experiment. To simplify the calculation process, the working system is considered to be adiabatic, and the thermal damage on aluminum surface is assumed to be hemisphere. The surface material will be gasified and the thermal damage is formed. The expansion work for aluminum from solid translated into gas can be expressed as follows:

$$W = p\Delta V = p\left(V_g - V_{sg}\right) \quad (10)$$

where, p is the ambient pressure; V_g and V_{sg} are the volume for aluminum foil at solid and gas state, respectively.

Considering the aluminum volume change ($V_{sg} >> V_g$), Eq. (10) can be simplified and given by the following:

$$W = pV_g = nR\Delta T = \frac{m}{M} R\Delta T \quad (11)$$

where, m is the gasified mass, M is the relative molecular mass of aluminum, R is the gas constant, ΔT is the temperature rise.

$$m = \frac{2}{3}\pi r^3 \rho_{Al} \quad (12)$$

where, r is the radius of hemisphere, ρ_{Al} is the density of the material.

The work of the bubble collapsing to aluminum surface is obtained as follows:

$$U = W + n\Delta T\Delta S = W + \frac{m}{M}\Delta T\Delta S \quad (13)$$

where, ΔS is the difference value of aluminum between solid state and gas state.

Taken the material characteristics into consider, the vaporization heat from aluminum gasifying can be expressed as follows:

$$Q_p = U + p\Delta V = 2pV_g + n\Delta T\Delta S \quad (14)$$

Based on the energy conservation, the energy produced by the bubble collapse is equal to the vaporization heat of aluminum, and it can be expressed as follows:

$$E_a = \frac{4}{3}\pi R_s^3 \rho_{v0} \frac{B_v}{\gamma - 1}\left(T_c - T_0\right) = 2pV_g + n\Delta T\Delta S = Q_p \quad (15)$$

Based on the Eq. (15), the temperature change for aluminum surface can be expressed by the following:

$$\Delta T = \frac{4\pi R_s^3 \rho_{v0} B_v \left(T_c - T_0\right) M/(\gamma - 1)}{4\pi r^3 \rho_{Al} R + 2\pi r^3 \rho_{Al} S} \quad (16)$$

3.4. EXPERIMENTAL PREPARATION

The temperature produced in the honing zone exerts an important influence on UVH. The thermal damage caused by the cavitation bubble collapse is significant and affects product surface quality. The experiment is conducted in an ultrasonic drilling machine to verify the simulation results (Fig. 3(a)). A drilling machine is used because UVH hinders the proper observation view of the machining process and results and unlike in a drilling machine, the ultrasonic amplitude at the processing postition in UVH is approximate. Therefore, a drilling machine should be used to replace the honing process. Purified water is chosen as the cooling liquid, and ultrasonic cavitation is developed in water. In the experiment, a glass container is used to survey the cavitation process.

For the investigation, an aluminum foil is chosen as the machining workpiece to properly observe the results. In preparing some test samples for various shapes (Fig. 3(b)), several samples are made for each shape in case a certain sample is destroyed.

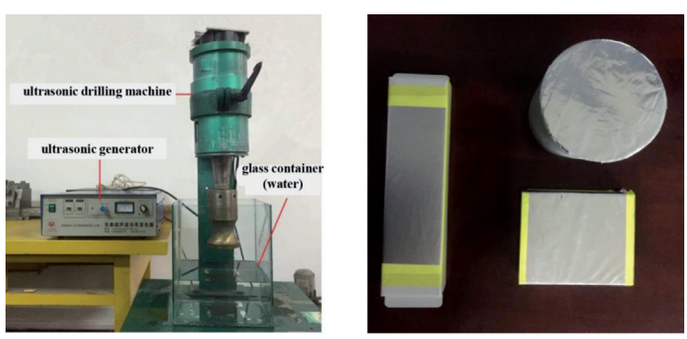

(a) (b)

Fig. 3: Experiment preparation. (a) Fundamental experiment device. (b) Different samples for various shapes

4. RESULTS ANALYSIS

4.1. NUMERICAL SIMULATION

Eq. (2) can be computed using logical values. Bubbles behave different motions under different parameters. This section discusses this type of behavior in detail.

In Eq. (2), the motor process of the cavitation bubble can be obtained by choosing and modifying the honing parameters. The following values are assumed for further simulation:

d = 47 mm, f = 18.6 kHz, ρ = 1,000 kg/m^3, σ = 728 × 10^{-2} N/m, p_0 = 1 × 10^5 Pa, κ = 1.4, p_v = 2.33 × 10^3 Pa, μ = 0.839 × 10^{-3} Pa·s.

Table I shows values of the remaining parameters.

Table I: Variable parameters in UVH

Parameter (Units)	Symbol	Value
Rotation speed of the honing head (r/min)	n	80, 110, 160, 200, 240, 310
Ultrasonic wave vibration amplitude (μm)	A	5-10
Reciprocation speed of oilstone (m/s)	v_a	0.05-0.4
Honing pressure (MPa)	p_h	0.24-1.5
Initial bubble radius (μm)	R_0	10, 15, 20, 30, 50
Ultrasonic wave stress amplitude (MPa)	p_a	0.797-2.058

4.1.1. Rotation speed of the honing head

Fig. 4 shows that the bubble breaks at a certain point after a series of oscillations. For a slow rotation speed, the bubble vibrates fiercely but presents a steady oscillation when the speed exceeds 120. A large amount of energy is collected inside the bubble. When the bubble inflates to a certain extent, it collapses and causes energy spraying. Furthermore, the maximal radius (~44 mm) can reach 45 multiples relative to the initial. At the same time, the bubble expansion time changes under different speed levels. When the speed quickly increases, the decrease rate of expansion time also increases. The figure shows that $n = 60$ equates to an expansion time of 45, $n = 80$ equates to an expansion time of 28, and $n = 100$ equates to an expansion time of 7.

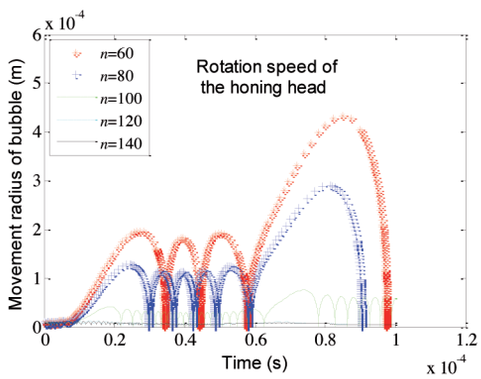

Fig. 4: Bubble movement radius under the rotation speed of the honing head
Parameter conditions: A = 5μm, v_a = 0.2 m/s, p_h = 0.24 MPa, R_0 = 10 μm, p_a = 1.2 MPa

4.1.2 Ultrasonic wave vibration amplitude

Different types of behavior are shown for the ultrasonic wave vibration amplitude in Fig. 5. The bubble is in a state of constant oscillation, and the radius shows an increasing trend. At the beginning, the oscillation is gentle within 0.2 × 10^{-4} s, and the movement trip of the bubble radius is sparse. However, the oscillation becomes severe when the trip overlaps and accumulates. Finally, the bubble cracks when enough energy is provided, and the radius expansion multiple is approximately 0.6.

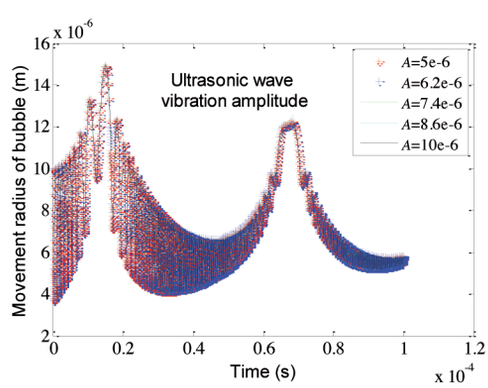

Fig. 5: Bubble movement radius under the ultrasonic wave vibration amplitude
Parameter conditions: n = 120, v_a = 0.2 m/s, p_h = 0.24 MPa, R_0 = 10 μm, *pa* = 1.2 MPa

4.1.3 Reciprocation speed of oilstone

A slow expansion is noted for the reciprocation speed of the oilstone shown in Fig. 6, and the bubble movement is similar to the rotation speed of the honing head. The difference is that the bubble collapses after several oscillations for every available parameter value. Otherwise, the radius enlargement factor decreases with reciprocation speed increasing. In this case, the maximal multiple exceeds approximately 45, and the minimal approach is 10. The bubble cracks at approximately 1 × 10^{-4} s, and the energy is accelerated to the extreme capacity. Moreover, the bubble oscillates before collapsing, and the vibration frequency increases with the speed increasing.

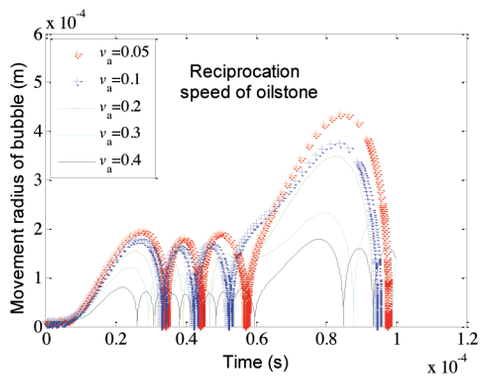

Fig. 6: Bubble movement radius under the reciprocation speed of oilstone
Parameter conditions: n = 120, *A* = 5 μm, p_h = 0.24 MPa, R_0 = 10 μm, *pa* = 1.2 MPa

4.1.4 Initial bubble radius

The change of the initial bubble radius fiercely generates bubble movement and accelerates bubble inflation (Fig. 7). The bubble magnification time of every initial radius approximately ranges from 6 to 16, which is smaller than that of the above parameters. Moreover, the maximal movement radius occurs before the collapse. The cavitation bubble is under a constant oscillation state. The energy inside the bubble is relevant to the initial radius. When the radius increases, more energy is needed to reach bubble collapse.

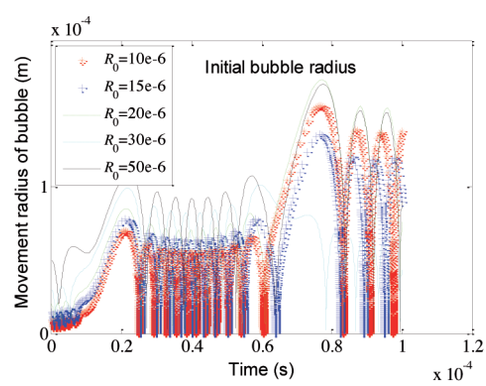

Fig. 7: Bubble movement radius under the initial bubble radius
Parameter conditions: n = 120, *A* = 10 μm, v_a = 0.4 m/s, p_h = 0.24 MPa, *pa* = 1.2 MPa

4.1.5 Ultrasonic wave stress amplitude

The apparent difference of bubble movement radius is shown for the ultrasonic wave stress amplitude (Fig. 8). Stationary vibration is the main motion mode when the amplitude is low. With the amplitude increasing, the bubble shows either single or multiple vibrations. When the amplitude increases to a value above 1.7 × 10^6 MPa, the bubble cracks after only one oscillation because the bubble collapses directly when the wave stress exceeds a certain value.

4.1.6 Honing pressure

Honing pressure is the force that presses the oilstone tightly to the workpiece and is the main reason for the grinding heat

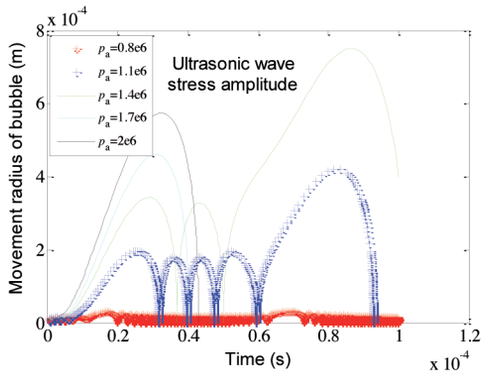

Fig. 8: Bubble movement radius under the ultrasonic wave stress amplitude
Parameter conditions: n = 120, *A* = 10 µm, v_a = 0.4 m/s, p_h = 0.24 MPa, R_0 = 15 µm

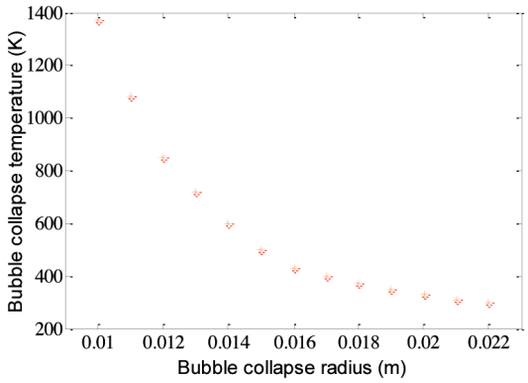

Fig. 10: Relation between bubble collapse radius and collapse temperature

production. With honing pressure increasing, bubble movement intensifies and becomes stable thereafter. Fig. 9 shows that the bubble immediately cracks after a single vibration when the honing pressure is low, whereas it does not quickly crack when the pressure reaches 0.82 × 10^6 MPa. If the value further increases, the bubble stabilizes in micro-vibration, and the radius maintain unchanged. For the other values, the bubble swells at the beginning and collapses later. The maximal radius is approximately 37 times as large as the initial radius.

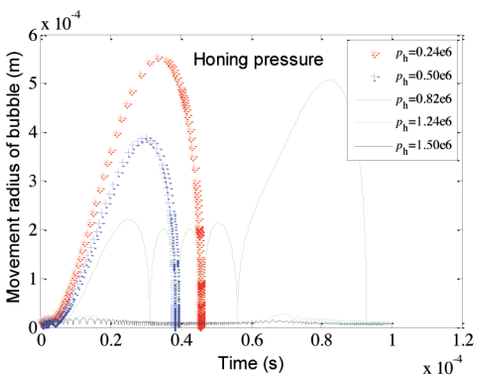

Fig. 9: Bubble movement radius under the honing pressure
Parameter conditions: n = 120, *A* = 10 µm, v_a = 0.4 m/s, R_0 = 15 µm, p_a = 1.5 MPa

The cavitation bubble maintains an oscillation or a steady vibration state before cracking in terms of most parameters. The movement radius changes for different conditions. Figures 4-9 show that the collapse radius is approximately 100 - 220 µm.

4.2. CAVITATION BUBBLE COLLAPSE TEMPERATURE

Based on the discussion in the section 3.2, the expression of bubble collapse temperature is shown in Eq. (9). It is simulated and shown in Fig. 10. The collapse temperature decreases when the bubble crack radius increases, and the gradient descend is rapid when the crack radius is small. The lowest temperature is approximately 300 K, and the highest temperature is 1,400 K. Furthermore, the temperature decreases from 1,380 K to 500 K when the crack radius increases only by 0.004. This result indicates that a smaller bubble collects more energy than a bigger bubble does, because a small bubble exhibits strong blastability for the same amount of energy. The bubbles are in a steady state with a slightly increasing radius, and they show a slight inflation. Therefore, the collection energy is only enough to support the bubble collapse, but it is insufficient to sustain the bubble to develop a micro-jet.

4.3. EXPERIMENTAL RESULTS DISCUSSION

An experiment was conducted to verify the theoretical analysis. In the experiment, the sample is placed in a glass container at a proper position for processing. The sample should be machined for several different heights and minutes to compare the results, but only a fixed position is chosen in this experiment (the distance is approximately 5 mm from the machining head to the workpiece). The sample is taken after machining for several seconds to observe the foil surface with a microscope. Given that the aluminum foil is thin, it can be easily worn down during machining. Therefore, several samples should be prepared because the result reveals the same pieces. For different working time, the surface behavior is apparently disparate from that shown in Fig. 11. As the samples are destroyed during processing, different results are observed in the samples.

Fig. 11 shows that the cavitation is unapparent from the beginning to 5 s. This condition can be explained by the fact that it takes some time for cavitation to occur and that several seconds is needed for the ultrasonic wave to transmit from the supersonic generator to the booster. After 10 s, apparent heat damage can be observed. Furthermore, the cavitation erosion is distributed uniformly and is apparently distinguishable from the cavitation erosion at 5 s. This result also shows that the ultrasonic cavitation occurs distinctly and intensively. Given the machining instability, the samples may not have the same shapes to reflect the result. At this point, the cavitation erosion is remarkable. The effect of the

(*a*) 5 *s* (*b*) 10 *s* (*c*) 15 *s*

Fig. 11: Observation results for different machining time

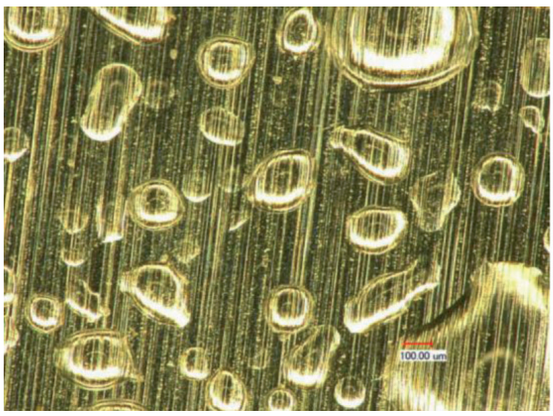

(a) Two-dimensional picture

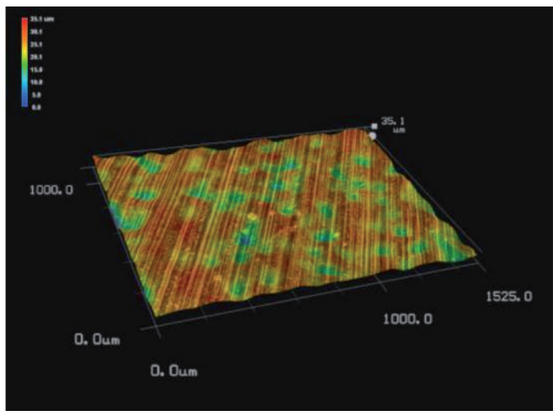

(b) Three-dimensional topography

Fig. 12: Observed figure for the aluminum foil in ×200 magnification

phenomenon is obvious after 15 s. The bubble is observed with a microscope for further investigations.

Fig. 12 shows the cavitation damage on the aluminum foil surface under a magnification of ×200. A variety of cavitation erosions with different shapes are existed on the surface. This result indicates that the energy in every bubble is disparate. Thus, the damage to the aluminum foil samples obviously differs. The 3D topography shows the size and the depth controlled by the energy are different. A set of fundamental parameters is chosen for the experiments. The bubble collapse damages the aluminum foil surface and causes cavitation erosion. In further analysis, thermal damage is assumed to be a hemisphere.

Base on the Eq. (16) and the model of section 3.2, the cavitation bubbles of different radius and shapes are formed in honing zone, then with bubbles collapsing, the diverse energy with high-temperature and high-pressure is released. When the experiment is completed, obvious variously thermal micro-pits which have different shapes and depths are shown on aluminum surface as shown on Fig. 12(*a*). In this study, the micro-pits are assumed to be hemisphere. From Fig. 12(*a*), the hemisphere radius of micro-pits on aluminum foil surface can be measured, and the material gasified temperature can be calculated by Eq. (16). Fig. 13 shows temperature change for the different micro-pits. It can be seen that the energy increases with the aluminum gasification volume increasing. Compared with the bubble collapse temperature (Fig. 10), the temperature rise of aluminum foil surface is several times as high as the collapse temperature of a single bubble. The reason is that the ultrasonic cavitation is a mass bubble phenomenon in experiment, and the surface is affected by several different bubbles. For different bubbles, the energy inside it is various, so there are diverse shapes for thermal damage.

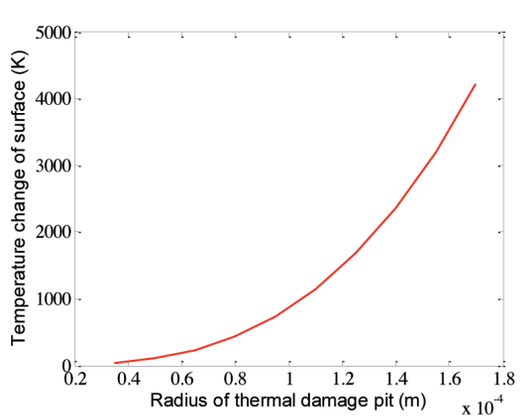

Fig. 13: Relation between thermal damage pit and temperature change

The thermal damage on the aluminum foil surface is obvious under some parameter conditions. In UVH, the thermal effect of bubble collapse is detrimental to the quality of workpieces, but cavitation is common in UVH. Thus, a reasonable parameter condition is needed to induce weakly cavitation for promoting the honing process. Given the limitation of experiment and measurement conditions, different test conditions should be tested to identify the ideal parameter condition. In this way, the quality of workpieces will be promoted and the working life of parts will be extended.

5. CONCLUSION

This study investigated the thermal damage of cavitation bubble for a workpiece in UVH. The cavitation bubble dynamics and thermodynamic equilibrium are applied to establish the bubble dynamic model and collapse temperature model. The effects of ambient and honing parameters are considered in the analysis. The simulation and experimental results indicate that the thermal damage of the cavitation bubble exerts an important influence on machining quality. The following are the main conclusions of this study.

(1) A dynamic model of cavitation bubbles in UVH is studied for the bubble movement trip by changing the honing parameter conditions. According to the simulation results, the bubble shows three different vibration patterns, including fierce oscillation until collapse, steady vibration, and direct crack after one oscillation. The bubble movement radius is 100-220 μm for all honing parameters.

(2) The bubble collapse temperature is presented. Numerical simulation indicates that the crack temperature decreases with the bubble collapse radius increasing and that the gradient decrease is rapid when the radius is small. The highest temperature exceeds 1,400 K, and the lowest is approximately 300 K (Fig. 10).

(3) The test results conducted on an ultrasonic drilling machine indicate that the thermal damage of the cavitation bubble on the aluminum foil surface is significant. The cavitation erosion caused by the bubble collapse is different, and these differences can be explained by the fact that the energy inside the bubble is distinguished. The data on bubble collapse temperature can be obtained with the model under a certain condition, which is compared with the temperature of the aluminum gasifying. The result shows that the experiment result is fairly well with the theory result.

The proposed model and method are suitable for simulating

the dynamic behavior of cavitation bubble, and they can improve UVH processing. Nonetheless, this study has some limitations. Only a fixed position is explored to observe the experiment, and the test results are not directly compared with the numerical results. A better comparison should be made in the future extensions of the study.

BIBLIOGRAPHY

[1] Zhu X J, Xu H J, Gao Y X, et al. "A new technology of improving surface quality of engine cylinder". *Key Engineering Materials*. 2008. Vol. 359-360. p.138-142. DOI: http://dx.doi.org/10.4028/www.scientific.net/KEM.359-360.138.

[2] Skladnev M F, Gun'Ko F G, Rubinshtein G L, et al. "Vacuum-cavitation stand for investigation of cavitation in hydraulic structures". *Hydrotechnical Construction*. September 1974. Vol. 8-9. p.837-842. DOI: http://dx.doi.org/10.1007/BF02380440.

[3] Tzanakis I, Lebon G S B, Eskin D G, et al. "Investigation of the factors influencing cavitation intensity during the ultrasonic treatment of molten aluminium"(In press). *Materials and Design*. 2016. p.979-983. DOI: http://dx.doi.org/10.1016/j. matdes.2015.11.010.

[4] Jia S, Zhang D, Xuan Y, et al. "An experimental and modeling investigation of aluminium-based alloys and nanocomposites processed by ultrasonic cavitation processing". *Applied Acoustics*. February 2016. Vol. 103. p.226-231. DOI: http://dx.doi.org/10. 1016/j.apacoust.2015.07.016.

[5] Harichandran R, Selvakumar N. "Effect of nano/micro B_4C particles on the mechanical properties of aluminium metal matrix composites fabricated by ultrasonic cavitation-assisted solidification process". Archives of Civil & Mechanical Engineering. January 2016. Vol. 16-1. p.147-158. DOI: http://dx.doi.org/10.1016/j.acme.2015.07.001.

[6] Lord Rayleigh O.M.F.R.S. VIII. "On the pressure developed in a liquid during the collapse of a spherical cavity". *Philosophical Magazine*. 1917. Vol. 34-200. p.94-98. DOI: http://dx.doi.org/10.1080/14786440808635681.

[7] Plesset M S. "The dynamics of cavitation bubbles". *Journal of Applied Mechanics*. September 1949. Vol. 16-3. p.277-282.

[8] Cai Jun, Huai Xiulan, Li Xunfeng. "Dynamic behaviors of cavitation bubble for the steady cavitating flow". *Journal of Thermal Science*. December 2009. Vol. 18-4. p.338-344. DOI: http://dx.doi.org/10.1007/s11630-009-0338-4.

[9] Hegedűs F, Hős C, Kullmann L. "Influence of heat transfer on the dynamic response of a spherical gas/vapor bubble". *International Journal of Heat & Fluid Flow*. December 2010. Vol. 31-6. p.1040-1049. DOI: http://dx.doi.org/10.1016 /j.ijheatfluidflow.2010.05.007.

[10] Dular M. "Hydrodynamic cavitation damage in water at elevated temperatures". *Wear*. January 2016. Vol. 346-347. P.78-86. DOI: http://dx.doi.org/10.1016/j.wear.2015.11.007.

[11] Liu B, Cai J, Huai X. "Heat transfer with the growth and collapse of cavitation bubble between two parallel heated walls". *International Journal of Heat and Mass Transfer*. November 2014. Vol. 78-11. p.830-838. DOI: http://dx.doi.org/10.1016/j.ijheatmass transfer.2014.07.050.

[12] Strotos G, Koukouvinis P, Thedorakakos A, et al. "Transient heating effects in high pressure diesel injector nozzles". *International Journal of Heat and Fluid Flow*. February 2015. Vol. 51. p.257-267. DOI: http://dx.doi.org/10.1016/j.ijheatfluidflow.2014.10.010.

[13] Zhou J, Wei, Hu J. "A novel approach for predicting thermal effects of gas cavitation in hydraulic circuits". *Energy*. April 2015. Vol. 83. p.576-582. DOI: http://dx.doi.org/10.1016/j.energy.2015.02.065.

[14] Zheng Z B, Zheng Y G, Sun W H, et al. "Effect of heat treatment on the structure, cavitation erosion and erosion-corrosion behavior of Fe-based amorphous coatings". *Tribology International*. October 2015. Vol. 90. p.393-403. DOI: http://dx.doi.org/10.1016/j.triboint.2015.04.039.

[15] Cai J, Huai X L, Yan R D, et al. "Numerical simulation on enhancement of natural convection heat transfer by acoustic cavitation in a square enclosure". *Applied Thermal Engineering*. July 2009. Vol. 29-10. p.1973-1982. DOI: http://dx.doi.org/10.1016/j.applthermaleng.2008.09.015.

[16] Zhao W G, Zhang L X, Shao X M. "Numerical simulation of cavitation flow under high pressure and temperature". *Journal of Hydrodynamics*. June 2011. Vol. 23-3. p.89-294. DOI: http://dx.doi.org/10.1016/S1001-6058(10)60115-1.

[17] Mohan B, Yang W, Chou S K. "Development of an accurate cavitation coupled spray model for diesel engine simulation". *Energy Conversion & Management*. January 2014. Vol. 77-1. p.269-277. DOI: http://dx.doi.org/10.1016/j.enconman.2013.09.035.

[18] Yang Y X, Wang Q X, Ts. K. "Dynamic features of a laser-induced cavitation bubble near a solid boundary". *Ultrasonic Sonochemistry*. July 2013. Vol. 20-4. p.1098-1103. DOI: http://dx.doi.org/10.1016/j.ultsonch.2013.01.010.

[19] Max Koch, Christiane Lechner, Fabian Reuter, et al. "Numerical modeling of laser generated cavitation bubbles with the finite volume and volume of fluid method, using OpenFOAM". *Computers and Fluids*. March 2016. Vol. 126. p.71-90. DOI: http://dx.doi.org/10.1016/j.compfluid.2015.11.008.

[20] Zhu X J, Guo C, Wang J Q, et al. "Dynamics modeling of cavitation bubble in the grinding area of ultrasonic honing". *Advanced Materials Research*. September 2013. Vol. 797. p.108-111. DOI: 10.4028/www.scientific.net/AMR.797.108.

[21] Guo C, Zhu X J, Wang J Q, et al. "Dynamical behaviors of double cavitation bubbles under ultrasonic honing". *Chinese Journal of Theoretical & Applied Mechanics*. June 2014. Vol. 46-6. p.879-886. DOI: http://dx.doi.org/10.6052/0459- 1879-14-108(in chinese).

[22] Liu G D, Zhu X J, Guo C. "Research on modeling and simulation of cavitation sound field in the grinding zone of the power ultrasonic honing". *ACTA ACUSTICA*. June 2013. Vol. 38-6. p.663-668. DOI: http://dx.doi.org/10.15949/j.cnki. 0371-0025.2013.06.003(in chinese).

[23] Cogné C, Labouret S, Peczalski R, et al. "Theoretical model of ice nucleation induced by acoustic cavitation. Part 1: Pressure and temperature profiles around a single bubble". *Ultrasonics Sonochemistry*. March 2016. Vol. 29. p.447-454. DOI: http://dx.doi.org/10.1016/j.ultsonch.2015.05.038.

[24] Cogné C, Labouret S, Peczalski R, et al. "Theoretical model of ice nucleation induced by acoustic cavitation. Part 2: Number of ice nuclei generated by a single bubble". *Ultrasonics Sonochemistry*. January 2016. Vol. 28. p.185-191. DOI: http://dx.doi.org/10.1016/j.ultsonch.2015.07.019.

[25] Schlender M, Spengler A, Schuchmann H P. "High-pressure emulsion formation in cylinder coaxial orifices: Influence of cavitation induced pattern on oil drop size". *International Journal of Multiphase Flow*. September 2015. Vol. 74. p.84-95. DOI: http://dx.doi.org/10.1016/j.ijmultiphaseflow.2015.04.004.

[26] Ye X, Yao X, Han R. "Dynamics of cavitation bubbles in acoustic field near the rigid wall". *Ocean Engineering*. November 2015. Vol. 109. p.507-516. DOI: http://dx.doi.org/10.1016/j.oceaneng.2015.09.045.

[27] Mahdi M, Ebhimi R, Shams M. "Numerical analysis of the effects of radiation heat transfer and ionization energy loss on the cavitation bubble's dynamics". *Physics Letters A*. June 2011. Vol. 375-24. p.2348-2361. DOI: http://dx.doi.org/10.1016/j. physleta.2011.04.026.

ACKNOWLEDGEMENT

The study was supported by National Natural Science Foundation of China(No. 51275490 and No. 50975265) and the Natural Science Foundation of Shanxi Province(No. 2013011024-5).